Spectral Analyses with the Standard Model. Part II: Wolf-Rayet Stars

W.-R. Hamann and L. Koesterke

Universität Potsdam, Germany

Abstract: The quantitative analysis of Wolf-Rayet type spectra requires non-LTE models for expanding atmospheres which became available in the last decade. Idealizing assumptions of the so-called standard model are spherical symmetry, homogeneity and stationarity. Synthetic spectra calculated under these assumptions are in general agreement with observation. However, specific observational facts (spectrum variability, X-ray emission) indicate that the standard assumptions are violated to some degree.

The standard model has been extensively applied to analyze the "classical", massive Wolf-Rayet stars of Population I. The galactic WN class has been studied comprehensively on the basis of helium-hydrogen models. The recent inclusion of their nitrogen lines by means of corresponding models confirms the results for WNL (i.e. late subtype WN) stars, while for part of the WNE (early subtype) stars a revision of the temperature scale is to be expected.

Some work remains to be done with the WC stars, which require models with carbon for their analysis. Only WC stars of intermediate subtype have been studied so far in the Pop. I domain. WC-type spectra are also shown by a considerable fraction of central stars of planetary nebulae. Recent spectral analyses of these low-mass stars, covering an extreme range of different subtypes, confirm the good experiences made with the standard model.

1 The Standard Model for WR Atmospheres

Wolf-Rayet (short: WR) type spectra are characterized by bright and broad emission lines. These lines are formed in a strong stellar wind which provides a large line-emitting volume. The width of the lines reflects the high streaming velocities of the radial outflow. Adequate modelling of WR atmospheres thus must account for their spatial extension, extreme non-LTE situations and supersonic velocity fields.

The available model atmospheres for WR stars are based on simplifying assumptions called the *standard model*, representing the most-idealized form of an expanding atmosphere. Spherical symmetry, together with stationarity and homogeneity, implies that the equation of continuity relates the velocity field $v(r)$ and the density structure $\rho(r)$ for a given mass-loss rate $\dot{M}$. Self-consistent hydrodynamic calculations for WR atmospheres are not yet available. Hence the velocity field must be adopted *ad hoc*. Usually the analytical form

$$v(r) = v_\infty \left(1 - \frac{R_*}{r}\right)^\beta \tag{1}$$

is adopted for its supersonic part, where the terminal velocity v_∞ and the exponent β are free parameters ($\beta = 1$ seems to be a good choice in most cases). The temperature structure follows from the assumption of radiative equilibrium. The stellar radius R_* needs a clear definition in the case of an extended atmosphere; we always refer it to an optical depth of 20 (Rosseland mean). T_* is the effective temperature referring to that radius.

Two independent codes for modelling WR atmospheres have been developed during the last decade, one by Hillier (see e.g. Hillier 1990) and one by the "Kiel group" – now resident in Potsdam and elsewhere (cf. Hamann & Wessolowski 1990). The basic features are the same in both codes. The stratification and the interplay between lines and continua are fully accounted for. The line radiation transfer is formulated in the co-moving frame of reference. Important effects which must be considered are the low-temperature dielectronic recombination and the frequency redistribution by electron scattering.

At present these models can handle fairly complex model atoms (e.g. He, C, N, O) with together a few hundred energy levels and more than thousand explicitly treated line transitions. Line blanketing by metals (e.g. iron, nickel) has been neglected so far, but its effect has been investigated by recent pilot studies (Schmutz 1994; Schaerer & Schmutz 1994). Additional to some modification of the UV continua, photon loss in strategic resonance lines by a fluorescence mechanism might affect the ionization structure significantly (Schmutz 1995 and this volume; Hillier, this volume).

The *standard model* calculations have been extensively compared to observed WR spectra, achieving reasonable agreement in general. However, certain limitations of the *standard model* are obvious. Spectral variability, polarization, or the emission of X-rays are not predicted. Clearly the assumptions of stationarity and homogeneity are violated to some degree, and the stellar winds are actually structured with clumps and shocks. First-order approximations accounting for inhomogeneous winds are discussed by Schmutz (1995 and this volume) and Hillier (this volume). Specific differences between calculated and observed WR spectra which are notoriously encountered might possibly not be due to deficiencies of the *standard model* assumptions, but rather to details of the modelling or unsuitable choices of the parameters (cf. Sect. 2).

2 Analyses, Results, Problems

For a quantitative spectral analysis, the observed spectrum is compared to synthetic spectra from model calculations. The model parameters (i.e. T_*, R_*, $\dot{M}$, v_∞, composition) are varied in order to achieve an optimum agreement. Model grids are required for an orientation in the parameter space and can be applied for coarse analyses. Corresponding diagrams with contours of constant line equivalent widths have been published for pure-helium models (WN stars) by Schmutz et al. (1989) and for helium-carbon models (WC stars) by Koesterke et al. (1992).

Schmutz et al. (1989) pointed out that the "absolute" parameters (e.g. L, $\dot{M}$, R_*) of a WR star cannot be derived definitely without the knowledge of its distance or absolute brightness. However, a purely spectroscopic parameter that can be obtained from a spectral analysis of an expanding atmosphere is the "transformed radius" R_t which Schmutz et al. (1989) defined as

$$R_\mathrm{t} = R_* \left(\frac{v_\infty / 2500\,\mathrm{km\,s^{-1}}}{\dot{M} / 10^{-4}\,M_\odot\,\mathrm{yr}^{-1}} \right)^{2/3} . \tag{2}$$

R_t is independent from the adopted distance of the star and thus plays in expanding atmospheres the role of $\log g$ in the static case. In order to establish the stellar radius, mass-loss

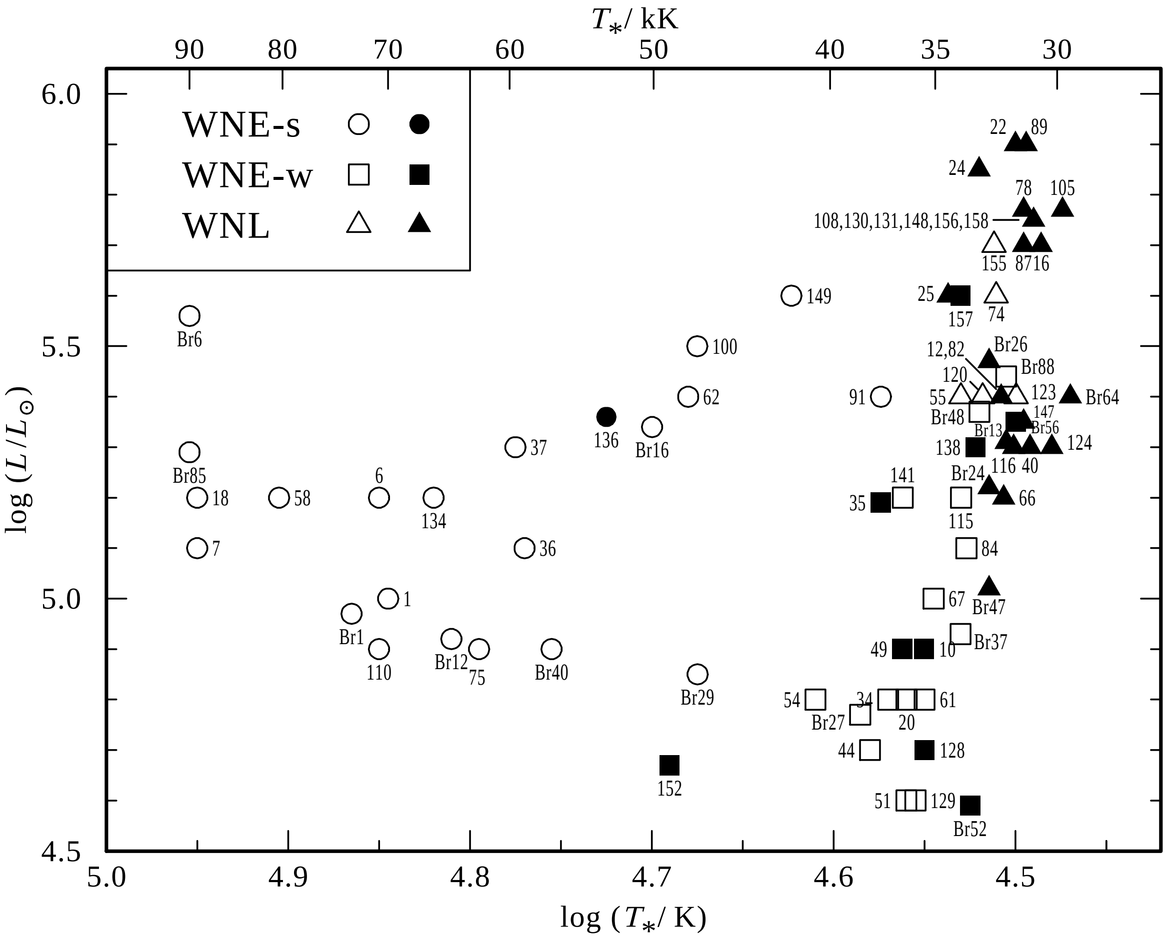

Figure 1: Hertzsprung-Russell Diagram of WN stars according to *standard model* analyses of their helium and hydrogen spectrum. The effective temperature T_* displayed at the abscissa refers to the radius where the Rosseland optical depth is 20. Different subclasses are distinguished by different symbol shapes (see inlet). Filled symbols indicate WN stars with detectable hydrogen, while open symbols stand for hydrogen-free atmospheres. The Galactic stars are identified by their WR number (catalogue by van der Hucht et al. 1981), while objects from the LMC are identified by "Br" numbers according to Breysacher (1981).

rate and luminosity, additional knowledge of the distance (or, equivalently, the absolute visual brightness or another absolute quantity) is prerequisite.

Fortunately, for many of the Galactic WN stars their distance is known from their membership in open clusters or associations. For the rest of them suitable calibrations can be suggested. In the case of Galactic WC stars there is less knowledge of distances. Studies of WR stars in the LMC have the great advantage to escape from this problem.

2.1 WN stars

The WN spectra are arranged in a subtype sequence (Smith 1968) according to the degree of ionization of nitrogen as reflected by the ratios between the strength of characteristic emission lines. Subtypes WN2 to WN6 are called "early" (WNE), while WN7 to WN9 are "late" (WNL). For WNE stars it is useful to distinguish between spectra with strong (WNE-s) and weak (WNE-w) emission lines. Smith et al. (1996) recently introduced slightly different criteria and notations for the discrimination of weak and strong lined stars, and add an "h" to the designation if the presence of hydrogen is reflected by an oscillating He II Pickering decrement. An almost complete atlas of Galactic WN spectra is electronically accessible (Hamann et al. 1995b).

2.1.1 Analyses of the helium spectrum

Almost all of the Galactic WN stars have been analyzed quantitatively by comparing their spectra with pure-helium models (cf. Hamann et al. 1995a, and references therein). If an alternating He II Pickering decrement indicates the presence of hydrogen, helium-hydrogen models were applied for its quantitative abundance determination. 19 WN stars in the LMC were analyzed with pure-helium models by Koesterke et al. (1991), and the hydrogen presence was rated qualitatively by Smith et al. (1996), while a quantitative determination is just in progress (Koesterke et al., in preparation).

The empirical HRD of the WN stars as obtained from these helium-hydrogen analyses is shown in Fig. 1. The WNL stars are found to arrange themselves in a vertical strip at 30 ... 35 kK, which is continued towards lower luminosities by the WNE-w subclass. The WNE-s stars populate a wide temperature range from 50 ... 90 kK and intermediate luminosities. There is no obvious difference in the HRD distribution between the WN stars in our Galaxy and in the LMC. Especially, the LMC stars are not more luminous on the average – contrary to the prediction of standard evolutionary calculations.

The abundance determinations confirmed that all WN stars are hydrogen deficient (Hamann et al. 1995a). In fact, 53% of the Galactic WN sample (33 out of 62 studied stars) are even free of hydrogen within the detection limits. The occurrence of hydrogen is restricted to those WN stars with lowest stellar temperatures (30 ... 38 kK, with two exceptions), comprising most WNL stars and part of the WNE-w subgroup (filled symbols in Fig. 1). For those WN stars showing hydrogen the typical abundance ranges between 10% and 30% (hydrogen mass fraction). A small group of four WN7 stars (WR 22, 24, 25, 87) with very high luminosity ($> 10^{5.6} L_\odot$) has outstandingly high hydrogen mass fractions (40 ... 53%).

2.1.2 Analyses regarding nitrogen

The next step of sophistication was the inclusion of nitrogen into the model calculation, which is not a trivial task because of the complexity of this atom. The nitrogen lines of WR 6 were studied first in the pilot paper by Hillier (1988). Much later a He-N analysis of WR 136 was presented by Hamann et al. (1994), while Crowther et al. (1995a,b) re-analyzed together ten Galactic WNL stars. In the latter cases the previous helium-hydrogen results were fully confirmed, while a slightly higher temperature and luminosity was obtained for the WN6-s subtype WR 136 (see Fig. 2). Crowther (1995a) also analyzed four WN 9-10 stars in the LMC which are included in Fig. 2.

Significantly different parameters were obtained, however, when re-analyzing WNE-w with regard to their nitrogen lines. WR 128 (WN4-w) and WR 152 (WN3-w) have been revisited by Crowther et al. (1995c) and are found to be considerably hotter and more luminous than previously determined (cf. Fig. 2). There are three Galactic WN stars of earliest subtype (WN2-w and WN3-w) which do not show any He I lines and were therefore not accessible to an analysis by helium lines alone. These three stars now were also investigated by means of their nitrogen lines (WR 46: Crowther et al. 1995c; WR 2 and WR 3: preliminary results from Hamann et al., in preparation) and are found to be extremely hot, as suggested from the total absence of neutral helium.

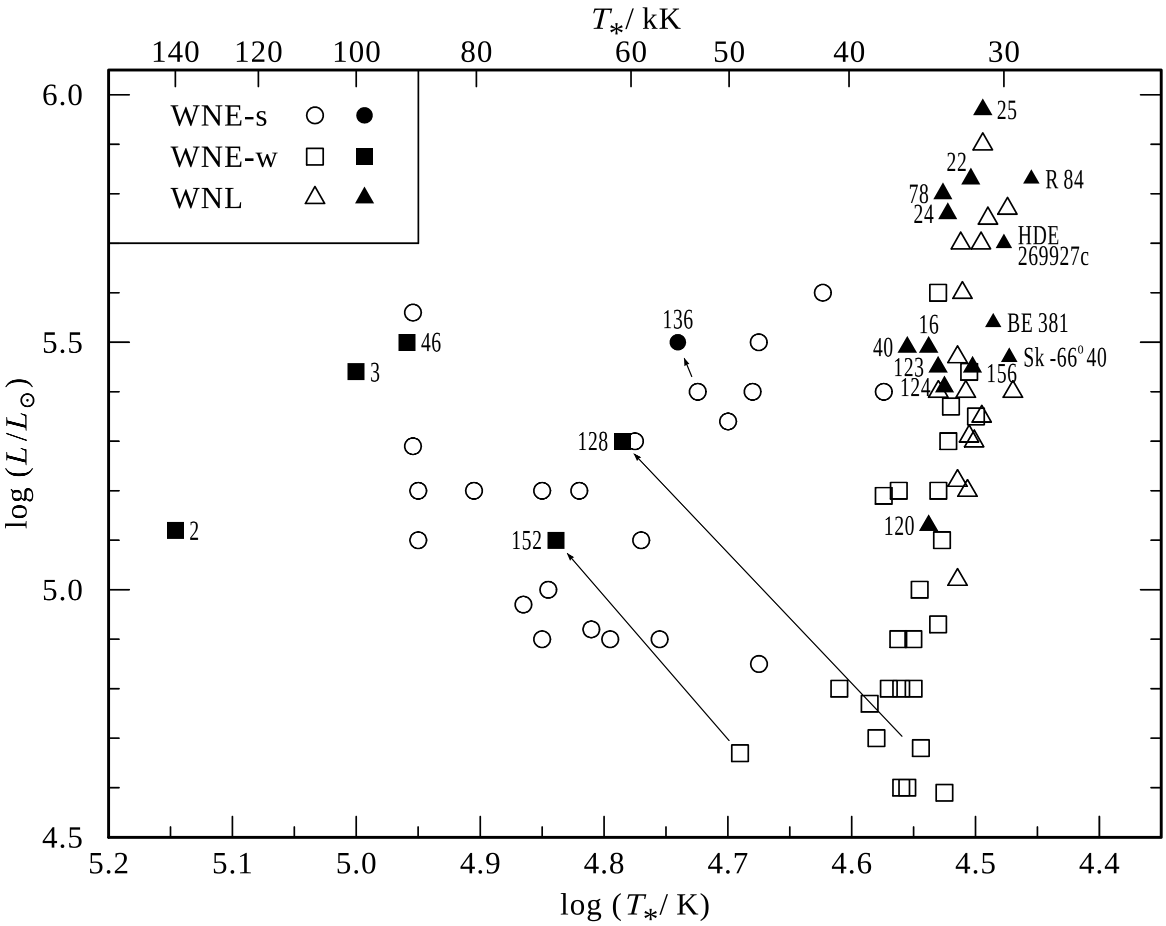

Figure 2: Hertzsprung-Russell Diagram of WN stars. Parameters obtained from analyses including nitrogen are emphasized by filled symbols and identification labels. Open symbols refer to helium analyses (cf. Fig. 1). Different subclasses are again distinguished by different symbol shapes (see inlet). The Galactic stars are identified by their WR number (catalogue by van der Hucht et al. 1981). Considerably different results are obtained in the case of re-analyzed WNE-w stars, as indicated by arrows. In contrast, the WNL parameters are confirmed.

In the HRD shown in Fig. 2 the results obtained from nitrogen analyses are emphasized by filled symbols and identification labels. They suggest a qualitatively different picture, if we speculate that *all* WNE-w stars will move to the upper left in the same way as WR 128 and WR 152 when being re-analyzed. Now the WN stars seem to arrange in a horizontal strip at $\log L/L_\odot = 5.3 \pm 0.2$. Only a few WNL stars are even brighter (up to $10^6 L_\odot$). The effective temperature T_* varies from about 30 kK for the WNL to more than 100 kK for the earliest WNE-w subtypes.

But how can it happen that pure-helium analyses are so much in error just for the WNE-w subclass? Let us explain this in some detail.

The fundamental parameters which determine the spectral appearance of an expanding stellar atmosphere are the effective temperature and the transformed radius (cf. Eq. 2). Therefore Schmutz et al. (1989) used contours of constant line equivalent widths in the $\log T_* - \log R_\mathrm{t}$ plane for a coarse spectral analysis (which might be refined subsequently by individual calculations adjusting also the secondary parameters). Schmutz et al. (1989) generated contour plots for the strategic lines He I 5876 and He II 5412, covering the temperature range between 30 and 90 kK. Essentially these contours are reproduced in Fig. 3. Given the measured equivalent

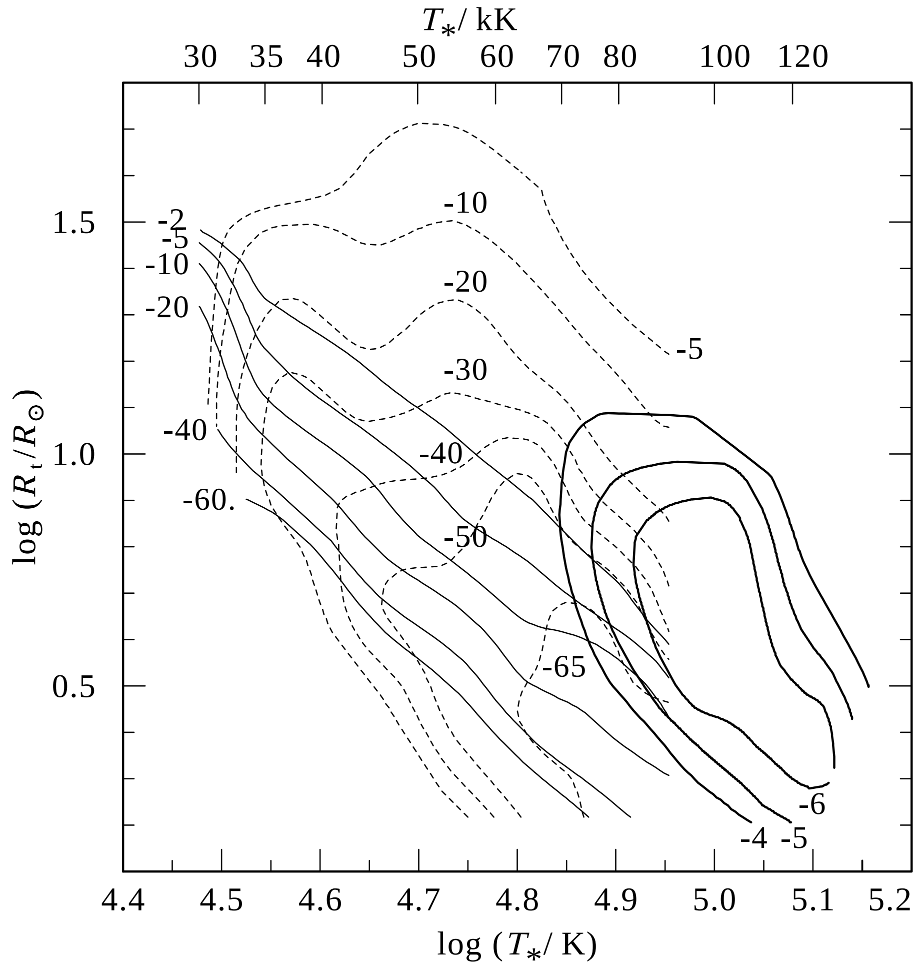

Figure 3: Contours of constant line equivalent widths (labels in Å) in the log T_*-log R_t plane for He I 5876 (thin solid line), He II 5412 (dashed) and N V 4933-4944 (thick line).

widths of an observed star, its parameters T_* and R_t can be read off from the intersection point of the corresponding contours.

A similar grid of models has been calculated recently (Koesterke et al., in preparation) with models including nitrogen. This grid has been extended to much higher temperatures (200 kK), because it turned out that hardly any N V lines became visible within the Schmutz et al. parameter range. However, the presence of N V lines is mandatory for WNE stars by definition of the early WN subtypes. In Fig. 3 the contours for the classification line N V 4933-4944 are shown from a part of this new model grid. It demonstrates that any WNE star with – per definition – visible N V 4933-4944 line (an equivalent width of -4 Å is indeed a typical value observed) must be located in the corresponding region at the lower right part of Fig. 3, i.e. at temperatures above 65 kK.

But what about the intersection point defining the helium solution? This question is not yet fully settled, but it seems that the He II contours can have a second intersection point at high T_*. In the nitrogen analyses presented so far the nitrogen and helium lines could be reconciled to some degree. If there remains some discrepancy between the low ions (He I, N III) which demand low stellar temperatures, and the high ions (N V) which lead to high T_*, this might be due to deficiencies within the *standard model* calculations (e.g. the hitherto neglection of metal line blanketing). More likely, those discrepancies may reflect the limitations of the *standard model* assumptions. The low effective temperatures could be correct, while the high ions are

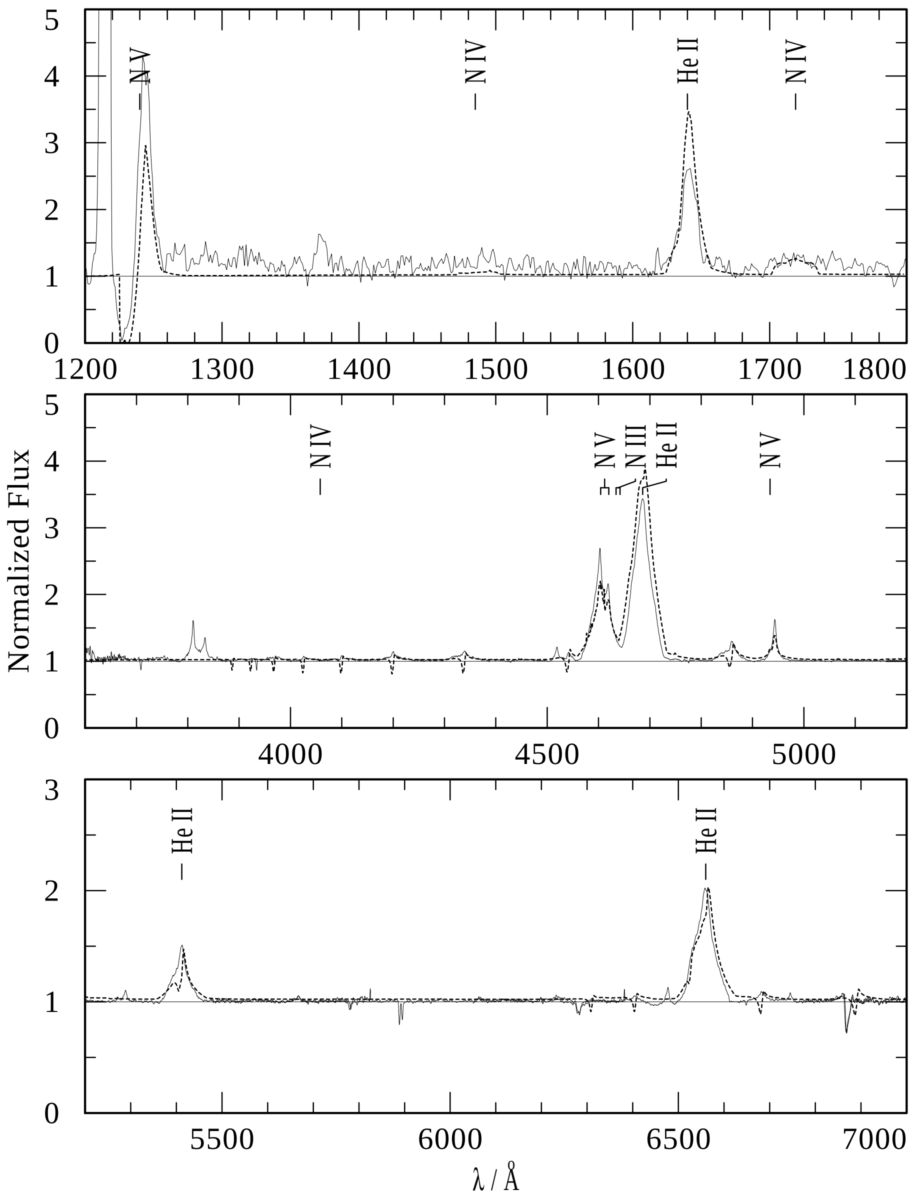

Figure 4: The spectrum of WR 46 (WN3pec-w), compared to a model (dashed line) with helium and nitrogen (1.5% by mass) having $T_* = 100\,\mathrm{KK}$, $R_\mathrm{t} = 10\,R_\odot$, $v_\infty = 2300\,\mathrm{km/s}$.

produced by shock heating and radiation. Alternatively, the higher T_* might be correct, and the low ions survive in the dense clumps of an inhomogeneous wind. Clearly these questions deserve further investigation.

In the case of the earliest WN subtypes, no discrepancies concerning the He I lines can occur because the latter are absent anyhow. Figure 4 displays a (preliminary) fit of WR 46 showing He II, N V and weak N IV lines which are all nicely reproduced by the model. The balance between N V and N IV is the basic diagnostic tool here.

The location of the re-analyzed WNE-w stars in the $\log T_* - \log R_\mathrm{t}$ plane is shown in Fig. 5. Two contours for N V lines roughly indicate the minimum temperature for the early subtypes. The picture now looks more complicated than previously from the helium analyses. The WNE-w stars now populate their own region, and at higher temperatures two different subclasses coexist, the WNE-s with low R_t (i.e. dense wind) and the WNE-w with weaker mass-loss. WR 2 appears like an high-temperature fellow of the WNL-WNE-s strip, rather than a member of

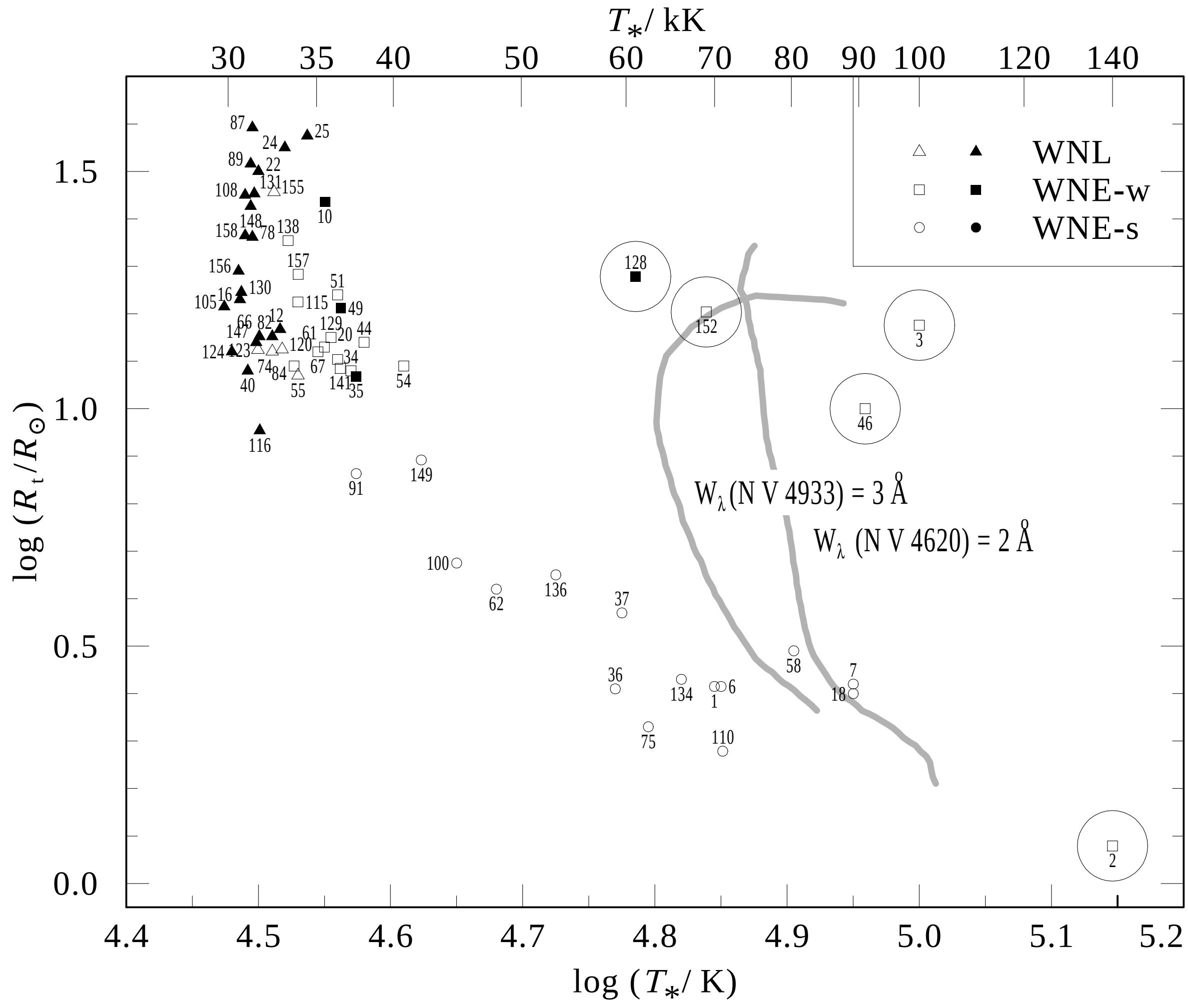

Figure 5: Locations of the WN stars in the $\log T_*$-$\log R_{\rm t}$ plane. The spectroscopic subclasses are distinguished by different symbol shapes (see inset). Filled symbols denote stars with hydrogen being detected in their spectra, while open symbols refer to stars without hydrogen. While most parameters are from helium-line analyses, the WNE-w stars analyzed from their nitrogen spectrum are encircled. Theoretical contours of constant line equivalent widths are given for two N V lines (shaded curves). According to these models, WNE stars must be located to the right of these lines in order to produce N V lines which are constitutive for this subclass.

the WNE-w subclass.

A further benefit from the nitrogen analyses is, of course, the gain of nitrogen abundances. Crowther et al. (1995a,b,c) determined the nitrogen, carbon and, in a few cases, even oxygen abundances for a couple of WN stars in the Galaxy and LMC (cf. Table 1). Hydrogen and nitrogen abundances are nicely anti-correlated (cf. Fig. 6). Very surprising is the outstandingly high oxygen content in the atmosphere of WR 46.

The "mixed" WN/WC type star WR 8 has been analyzed in detail by Crowther et al. (1995d). All WN *and* WC spectral features could be explained within one consistent model, i.e. without a binary assumption. Its chemical composition resembles that of a WN star, but with enhanced carbon and oxygen abundance ($\approx 6\%$ carbon by mass), while normal WN stars are poor of carbon (cf. Table 1).

Star	Type	Abundances (mass fractions)				Reference
		H [%]	N [%]	C [%]	O [%]	
WR 25	WN7abs	53	0.4	0.03	-	Crowther et al. 1995b
WR 24	WN7abs	44	0.7	0.05	-	Crowther et al. 1995b
WR 22	WN7abs	44	1.0	0.03	-	Crowther et al. 1995b
WR 156	WN8	27	1.7	0.20	-	Crowther et al. 1995b
WR 16	WN8	20	1.6	0.01	-	Crowther et al. 1995b
WR 128	WN4-w	14	1.4	0.06	0.08	Crowther et al. 1995c
WR 152	WN4-w	14	1.4	0.06	0.08	Crowther et al. 1995c
WR 40	WN8	15	1.7	0.01	-	Crowther et al. 1995b
WR 78	WN7	11	1.7	0.03	-	Crowther et al. 1995b
WR 124	WN8	13	1.2	0.03	-	Crowther et al. 1995b
WR 136	WN6-s	12	1.5	-	-	Hamann & Wessolowski 1994
WR 123	WN8	0	1.7	0.05	-	Crowther et al. 1995b
WR 46	WN3pec-w	0	2.1	0.05	0.24	Crowther et al. 1995c
WR 8	WN/WC	0	2.6	6	3	Crowther et al. 1995d
R 84	WN9	38	0.6	0.02	-	Crowther et al. 1995a
BE 381	WN9	33	0.6	0.04	-	Crowther et al. 1995a
HDE 269927c	WN9	30	0.6	0.04	-	Crowther et al. 1995a
Sk -66°40	WN10	46	0.3	0.08	-	Crowther et al. 1995a

Table 1: Chemical abundances in WN stars, as obtained from *standard model* analyses

2.2 WC stars

Analogously to the WN stars, Wolf-Rayet spectra of the carbon subclass are arranged in a subtype sequence from WC2 to WC12, depending on the strength of selected carbon and, as

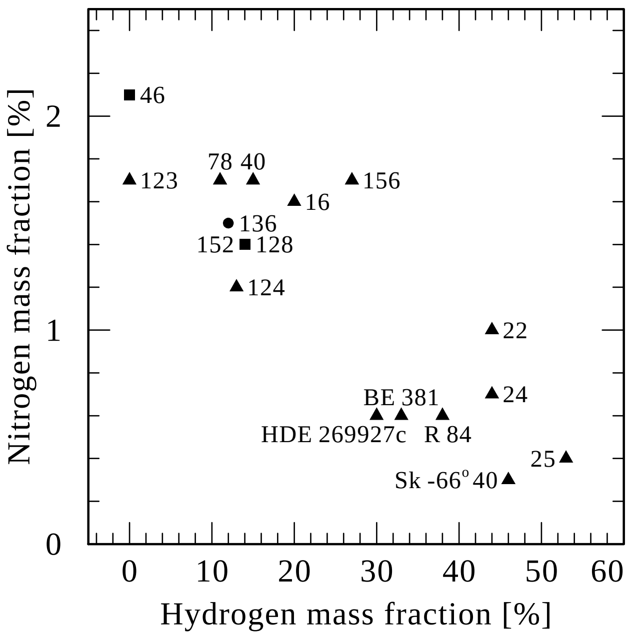

Figure 6: Hydrogen versus nitrogen abundance in WN stars, as obtained from *standard model* analyses (cf. Table 1). The spectroscopic subclasses are distinguished by different symbol shapes (see previous figures).

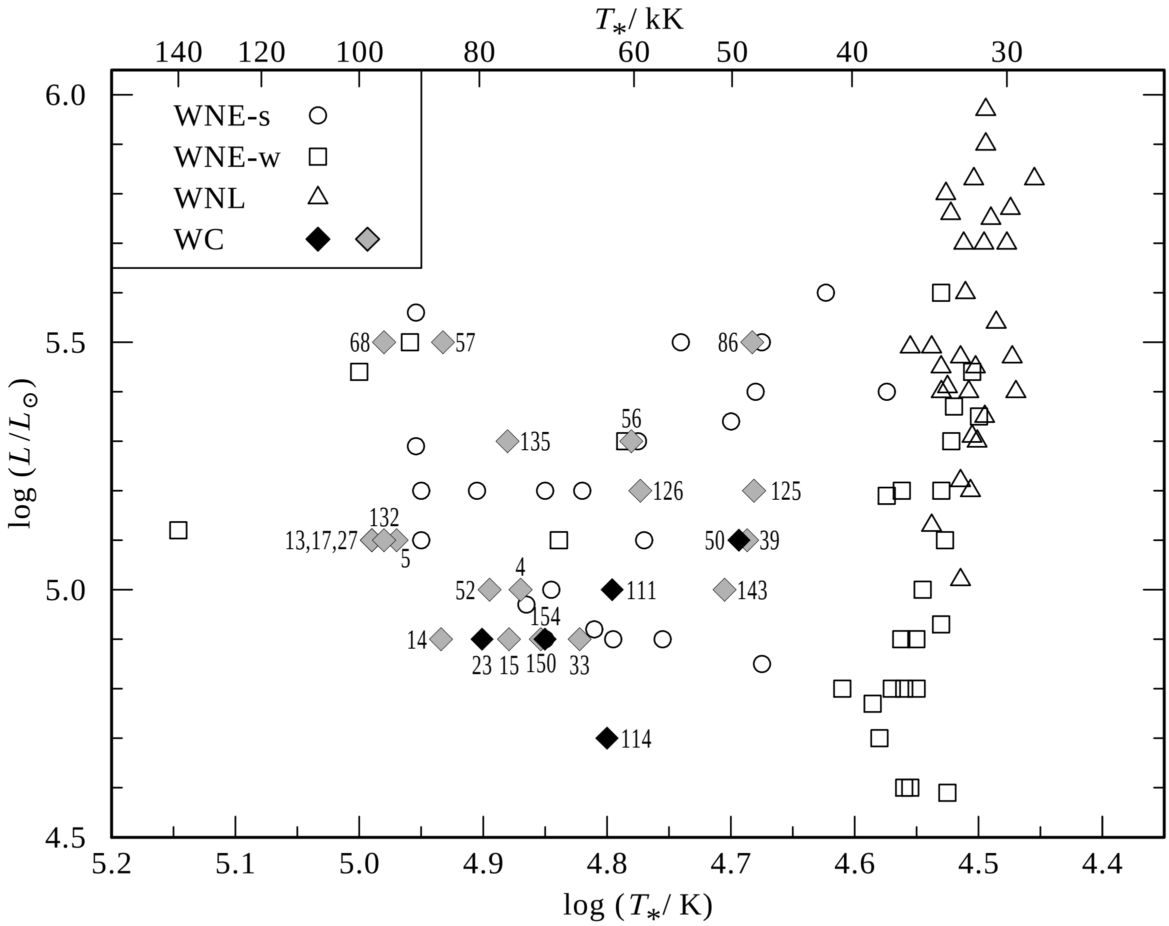

Figure 7: Hertzsprung-Russell Diagram of WC stars according to *standard model* analyses of their helium and carbon spectrum. The effective temperature T_* displayed at the abscissa refers to the radius where the Rosseland optical depth is 20. WC stars are represented by diamonds and labeled by their WR number (catalogue by van der Hucht et al. 1981). Black symbols denote stars with known distance, while for the other WC stars (shaded) the luminosities are more uncertain. Open symbols without labels refer to WN stars (cf. Fig.2).

secondary criteria, oxygen emission lines (van der Hucht et al. 1981, Méndez & Niëmela 1982, Hu & Bibo 1990). Subtype numbers up to WC6 are comprehensively termed as "early" (short: WCE), the rest as "late" (WCL). A uniform atlas of WC spectra has been published by Torres & Massey (1987).

Pilot analyses of the WC5 star WR 111 including carbon have been published by Hillier (1989) and Hamann et al. (1992). 25 Galactic WC stars of intermediate subtype (WC5 ... WC7) were analyzed by Koesterke & Hamann (1995) using helium-carbon models. The determination of absolute quantities (luminosities etc.) for WC stars is even harder than for WN stars, because there are only few WC stars in clusters or associations and hence almost all distances are uncertain. The obtained luminosities range from $10^{4.8}$ to $10^{5.5}\,L_\odot$, while T_* varies from 60 to 100 kK for these intermediate WC subtypes (Fig. 7). The carbon-to-helium mass ratio lies between 0.25 and 1.5 for the considered WC stars.

These analyses of WC stars by Koesterke & Hamann (1995) suffer from a similar problem as discussed in Sect. 2.1.2 concerning the WN analyses. When including oxygen into the models, the reproduction of the observed O VI lines requires higher temperatures (analogously to the N V lines in the case of WNE stars). Thus the WC stars should also be revisited in future

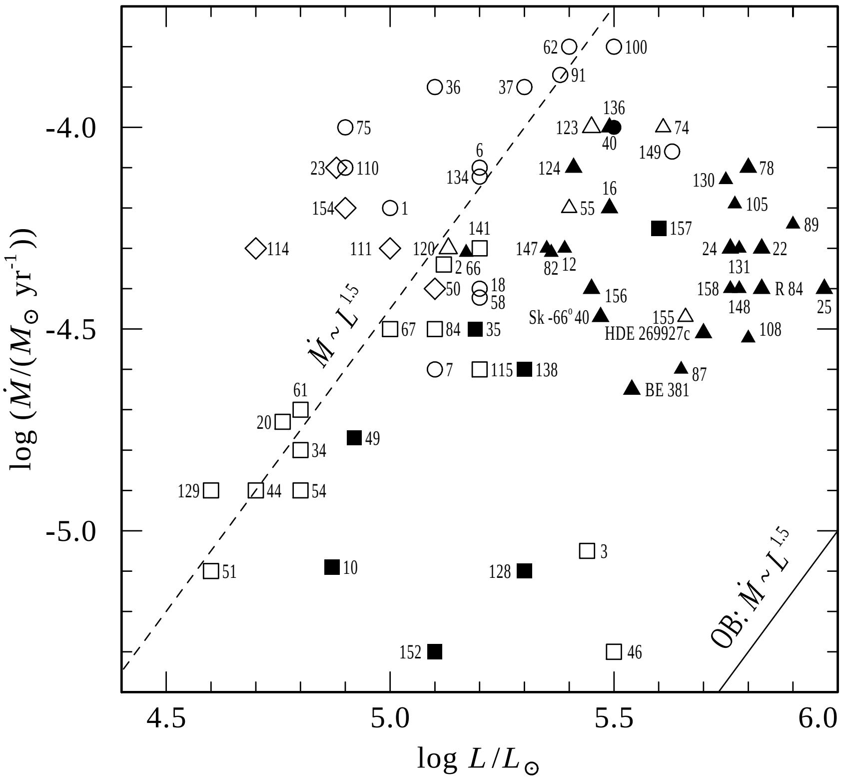

Figure 8: Mass-loss rates of WR stars versus luminosity, as obtained from the best available *standard model* analyses. The individual stars are labeled, plain numbers referring to the WR catalogue (van der Hucht et al. 1981). Triangles, squares and circles represent WNL, WNE-w and WNE-s stars, respectively. Five WC stars with well-established data are also represented (diamonds). Filled and open symbols indicate whether hydrogen is detectable or absent, respectively. The dashed line gives a tentative fit to the mass-loss rates of *hydrogen-free* WN stars, while those WN stars *with hydrogen* lie to the lower-right of that relation. The corresponding relation for OB stars is indicated at the lower-right corner.

work, using models with He, C and O. A corresponding study about WC4 stars in the LMC is in progress presently in Potsdam.

WC type spectra are also encountered in a considerable fraction of the central stars of planetary nebulae, although these stars obviously belong to an older population and are less massive and less luminous than their Pop. I relatives. A wide variety of subtypes has been analyzed with the Kiel/Potsdam models, fully accounting for He, C and O as recommended above (Leuenhagen & Hamann 1994; Leuenhagen et al. 1996; Koesterke & Hamann 1997a,b; Leuenhagen 1997). A wide parameter range is covered by these central stars. Their effective temperature T_* ranges from 20 kK (subtype WC12) to 140 kK (WC2). In all cases a reasonable agreement between observation and *standard model* calculations could be achieved.

3 Conclusions

At present the *standard model* analyses are the best that can be done to determine the parameters of Wolf-Rayet stars and their expanding atmospheres. There is a twofold interest in the results. First, it is not yet settled why the WR stars have mass-loss rates much higher than those of other hot (O or B type) stars, and higher than predicted by the theory of radiation

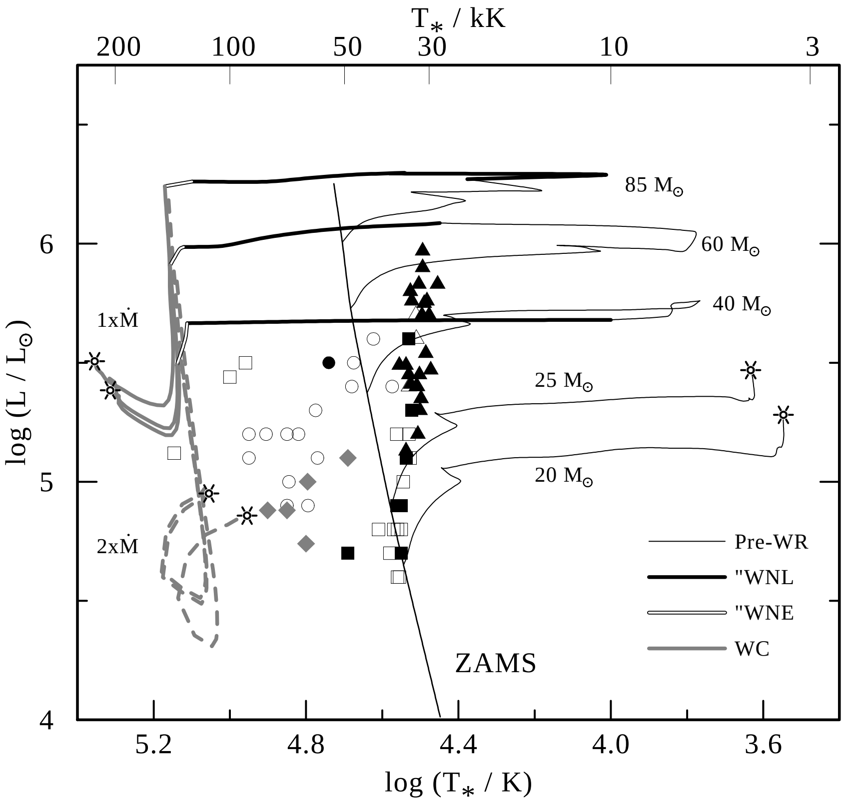

Figure 9: Hertzsprung-Russell Diagram. Discrete symbols indicate the locations of the Galactic WR stars as obtained from the best *standard model* analyses available (cf. Figs. 2 and 7). Triangles, circles or squares refer to WNL, WNE-s or WNE-w stars, respectively, while filled or open style indicates whether hydrogen has been detected or not. WC stars are represented by shaded diamonds. The theoretical tracks are taken from Schaller et al. (1992) (metallicity $Z = 0.020$) for different initial masses (labels). The tracks are for the "standard" assumptions on the mass-loss rates ("$1\times\dot{M}$"). Tracks for twice as strong mass-loss significantly differ only in the WC phase for which they are also shown ("$2\times\dot{M}$"). The evolutionary stages, defined according to the surface composition, are indicated by different drawing styles (see inlet). Note that the subclass definitions "WNL" and "WNE" used here refer to the presence or absence of hydrogen at the surface and thus can be directly compared with the representation of the observed stars by filled or open symbols. The effective temperature used as abscissa refers to the hydrostatic core radius in case of evolutionary tracks and to a Rosseland optical depth of 20 in the atmospheric models.

driven winds in its present state. Secondly, the WR stars are a key to the understanding of the evolution of massive stars.

The mass-loss rates of the *hydrogen-free* WN stars and the WC stars follow a tentative relation $\dot{M} \propto L^{1.5}$ (cf. Fig. 8). The corresponding relation established for OB stars has the same slope, but $\dot{M}$ is lower by a factor of 100, roughly, grazing only the lower right corner of Fig. 8. Even when speculating that those WNE-w stars not yet re-analyzed with nitrogen models will perhaps move to the right (up to 0.5 dex higher luminosities), the conclusion remains the same: WR stars have higher mass-loss than OB stars of same luminosity. Most remarkably, those WN stars with some atmospheric hydrogen are lying *between* the $\dot{M}$-L-relation for hydrogen-free WR stars and for the OB stars with their (more or less) normal surface composition. Even quantitatively, those WN stars with highest hydrogen mass fractions approach closest to the

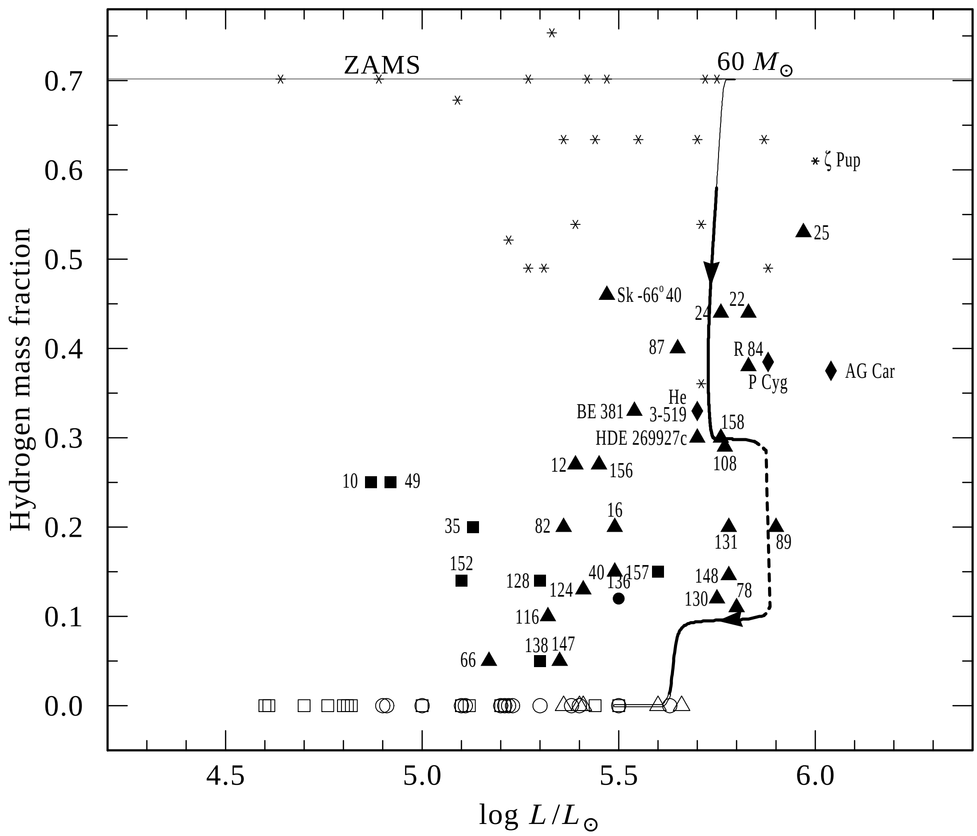

Figure 10: Hydrogen abundance versus luminosity for Galactic WN stars (labels: WR numbers according to the catalog by van der Hucht et al. 1981). Triangles, circles or squares refer to the different spectral types WNL, WNE-s or WNE-w, respectively. Open symbols crowding at zero hydrogen abundance indicate the luminosities of those WN stars showing no hydrogen signature. Small asterisks mark Galactic luminous OB stars analyzed by Herrero et al. (1992), only ζ Puppis being individually labeled. Black diamonds indicate three LBVs (P Cygni: Najarro et al. 1994; AG Car and He 3-519: Crowther & Willis 1994, Smith et al. 1994). A non-standard evolutionary track is shown (Langer et al. 1994) which accounts for mass-loss by violent pulsational instabilities. Different drawing styles along that track (cf. Fig. 9) refer to the predicted spectral appearance as "WNL" (heavy line), LBV (dashed), again "WNL" and finally "WNE" (double line).

OB relation. Mass-loss rates from WC stars gather above the dashed relation.

The empirical correlation between hydrogen deficiency and mass-loss rate might provide a key to understand the mass-loss mechanisms theoretically. Either, the chemical composition directly affects the driving mechanism (radiation pressure? pulsational instabilities?), or mass-loss rate and surface abundances change synchronously in the course of stellar evolution (e.g. caused by changing surface gravity or pulsational properties).

The standard evolutionary theory for very massive stars can in principle explain the formation of Wolf-Rayet stars when mass-loss is accounted for. However, the available theoretical calculations are partly in conflict with the results obtained from the spectral analyses as presented in the previous section (cf. Fig. 9). One problem concerns the luminosities. Even when suggesting that the lowest WNE-w luminosities from helium analyses are under-estimates as discussed in Sect. 2, the typical WN luminosity of $10^{5.3} L_\odot$ is less than predicted. A track for $30\,M_\odot$ would do well if it would return from the red side and reach the WN stage. For the most luminous WNL stars, the alternative scenario proposed by Langer et al. (1994) might apply.

Based on the assumptions of strong mass-loss in phases of pulsational instability, it relates O stars, Luminous Blue Variables and Wolf-Rayet stars in the evolutionary sequence O $\rightarrow$ Of $\rightarrow$ H-rich WN $\rightarrow$ LBV $\rightarrow$ H-poor WN $\rightarrow$ H-free WN $\rightarrow$ WC $\rightarrow$ SN.

The differences in temperature between tracks and observation (Fig. 9) do not mean a real contradiction, because different reference radii apply for the tracks (hydrostatic stellar radius) and the wind models ($\tau_{\mathrm{Rosseland}} = 20$), respectively. Nothing is known about the spatial extension of the subphotospheric ($\tau > 1$) but non-static layers (cf. the discussion in Hamann 1994).

A crucial test for evolutionary models is the comparison between predicted and observed atmospheric abundances. Figure 10 displays the hydrogen abundances in WN stars. The asterisks indicate corresponding results for luminous O and B stars, which are in most cases enriched in helium and nitrogen. Together with the LBVs, the diagram Fig. 10 is continuously populated from solar abundances to hydrogen-free composition. Evolutionary models predict, in contrast, quite sudden changes in surface composition due to steep chemical gradients. In order to produce the observed distribution abundances, internal mixing processes are probably required as a new physical input to the evolutionary modelling. The evolutionary track shown in Fig. 10 is for the alternative scenario by Langer et al. (1994) which connects the different classes on the basis of pulsation-driven mass loss.

Summarizing, spectral analyses of Wolf-Rayet stars with the *standard model* provide an important tool to investigate their parameters, evolutionary status and mass-loss mechanism.

References

Breysacher J., 1981, A&A Suppl. 43, 203

Crowther P.A., Willis A.J., 1994, Space Science Rev. 66, 85

Crowther P.A., Hillier D.J., Smith L.J., 1995a, A&A 293, 172

Crowther P.A., Hillier D.J., Smith L.J., 1995b, A&A 293, 403

Crowther P.A., Smith L.J., Hillier D.J., 1995c, A&A 302, 457

Crowther P.A., Smith L.J., Willis A.J., 1995d, A&A 304, 269

Hamann W.-R., 1994, Space Science Reviews 66, 237

Hamann W.-R., Wessolowski U., 1990, A&A 227, 171

Hamann W.-R., Leuenhagen U., Koesterke L., Wessolowski U., 1992, A&A 255, 200

Hamann W.-R., Wessolowski U., Koesterke L., 1994, A&A 281, 184

Hamann W.-R., Koesterke L., Wessolowski U., 1995a, A&A 299, 151

Hamann W.-R., Koesterke L., Wessolowski U., 1995b, A&A Suppl. 113, 1

Herrero A., Kudritzki R.P., Vilchez J.M., Kunze D., Butler K., Haser S., 1992, A&A 261, 209

Hillier, D.J., 1988, ApJ 327, 822

Hillier D.J., 1989, ApJ 347, 392

Hillier D.J., 1990, A&A 231, 116

Hu J.Y., Bibo E.A., 1990, A&A 234, 435

van der Hucht K.A., Conti P.S., Lundström I., Stenholm B. 1981, Space Sci. Rev. 28, 227

Koesterke L., Hamann W.-R., 1995, A&A 299, 503

Koesterke L., Hamann W.-R., 1997a, A&A (in press)

Koesterke L., Hamann W.-R., 1997b, in *Planetary Nebulae*, IAU Symp. 180, H.J. Habing and H.J.G.L.M. Lamers (eds.), in press

Koesterke L., Hamann W.-R., Schmutz W., Wessolowski U., 1991, A&A 248, 166

Koesterke L., Hamann W.-R., Wessolowski U., 1992, A&A 261, 535
Langer N., Hamann W.-R., Lennon M., Najarro F., Pauldrach A.W.A., Puls J., 1994, A&A 290, 819
Leuenhagen U., 1997, in *Planetary Nebulae*, IAU Symp. 180, H.J. Habing and H.J.G.L.M. Lamers (eds.), in press
Leuenhagen U., Hamann W.-R., 1994, A&A 283, 567
Leuenhagen U., Hamann W.-R., Jeffery C.S., 1996, A&A 312, 167
Méndez R.H., Niëmela V.S. 1982, in *Wolf–Rayet Stars*, Proc. IAU Symp. 99, C.W.H. de Loore & A.J. Willis (eds.), Reidel, Dordrecht, p. 457
Najarro F., Hillier D.J., Kudritzki R.P., Krabbe A., Genzel R., Lutz D., Drapatz S., Geballe T.R., 1994, A&A 285, 573
Schaerer D., Schmutz W., 1994, A&A, 288, 231
Schaller G., Schaerer D., Meynet G., Maeder A., 1992, A&AS 96, 269
Schmutz W., 1994, Space Sci. Rev. 66, 253
Schmutz W., 1995, in *Wolf-Rayet Stars: Binaries, Colliding Winds, Evolution*, K.A. van der Hucht and P.M. Williams (eds.), Proc. IAU Symp. 163, p. 127
Schmutz W., Hamann W.-R., Wessolowski U., 1989, A&A 210, 236
Smith L.F., 1968, MNRAS 140, 409
Smith L.J., Crowther P.A., Prinja R.K., 1994, A&A 281, 833
Smith L.F., Shara M.M., Moffat A.F.J., 1996, MNRAS 281, 163
Torres A.V., Massey P., 1987, ApJ Suppl. 65, 59